ADVANCED MATERIALS

DOI: 10.1002/adma.200701431

Organic Transistors Based on Di(phenylvinyl)anthracene: Performance and Stability**

By *Hagen Klauk*,* *Ute Zschieschang*, *Ralf T. Weitz*, *Hong Meng*,* *Fangping Sun*, *Geoffrey Nunes*, *Dalen E. Keys*, *Curtis R. Fincher*, and *Zhen Xiang*

The electrical performance of organic thin-film transistors (TFTs) often degrades when the devices are exposed to air. This is generally ascribed to the generation of trap states,[1] possibly as a result of the oxidation of the organic semiconductor.[2] One strategy to improve the stability of p-channel organic TFTs is the synthesis of conjugated semiconductors with a relatively large ionization potential.[3–8] However, most of the TFTs based on organic semiconductors with large ionization potentials reported up till now have shown carrier mobilities that are smaller than that of pentacene. Here, we report on a new organic semiconductor, di(phenylvinyl)anthracene (DPVAnt),[9] that combines large carrier mobility (similar to that of pentacene) with increased ionization potential and improved stability as compared to pentacene.

DPVAnt has been synthesized by a Suzuki coupling reaction between 2,6-dibromoanthracene and 4,4,5,5-tetramethyl-2-[2-phenylvinyl]-[1,3,2]dioxaborolane[9] with a yield of 85%. Pentacene has been purchased from Fluka. Both semiconductors have been purified by temperature gradient sublimation in a stream of inert gas. Cyclic voltammetry indicates a highest occupied molecular orbital (HOMO) energy of –5.4 eV for DPVAnt, as compared to –5.0 eV for pentacene. From UV-vis absorption spectroscopy we have determined an optical bandgap of 2.6 eV for DPVAnt and 1.8 eV for pentacene. These results are consistent with the general observation that molecules characterized by a smaller conjugated π-system have more negative HOMO energies and larger bandgaps.

Simple TFT test structures have been prepared on heavily doped silicon substrates (serving as the gate electrode) with a thermally grown SiO_2 gate dielectric. The dielectric surface has been treated with octadecyltrichlorosilane (OTS),[10] and the organic semiconductor has been vacuum deposited onto the substrate. Gold source/drain contacts have been thermally evaporated through a shadow mask (Fig. 1a). During the deposition of the semiconductor, the substrates are held at a temperature of 60 °C for pentacene and 80 °C for DPVAnt. The carrier mobilities extracted from the transfer characteristics measured in air are 1 $cm^2\ V^{-1}\ s^{-1}$ for pentacene and 1.3 $cm^2\ V^{-1}\ s^{-1}$ for DPVAnt (Fig. 1b). Both TFTs have an on/off current ratio of 10^7 and a subthreshold swing of 500 mV $decade^{-1}$. Perhaps the most striking differences between the two devices are the much more negative turn-on and threshold voltages of the DPVAnt transistor ($V_{turn\text{-}on}$ = –14 V, V_{th} = –16 V) as compared to the pentacene TFT ($V_{turn\text{-}on}$ = –2 V, V_{th} = –5 V). The exact reason for this difference is not known, but it may be related to the more negative HOMO energy of DPVAnt as compared to pentacene. As shown by the atomic force microscopy (AFM) images in Figure 1c and d, both semiconductors form well-ordered polycrystalline films, which is a prerequisite for obtaining large carrier mobilities.

For practical applications, a transistor structure with patterned gate electrodes and a low-temperature gate dielectric is required. Using a recently developed process[11] we have prepared pentacene and DPVAnt TFTs on glass substrates with Al gate electrodes coated by a thin gate dielectric based on a phosphonic acid self-assembled monolayer. The organic semiconductor has been vacuum deposited, and the gold source/drain contacts have been thermally evaporated. All the layers have been patterned using manually aligned shadow masks. Figure 2 shows the current–voltage characteristics of pentacene and DPVAnt TFTs with channel lengths of 20 μm and channel widths of 100 μm recorded in air shortly after device fabrication. The TFTs have essentially the same mobility (pentacene: 0.4 $cm^2\ V^{-1}\ s^{-1}$, DPVAnt: 0.3 $cm^2\ V^{-1}\ s^{-1}$), on/off current ratio (10^7), and subthreshold swing (100 mV $decade^{-1}$). Again, the turn-on and threshold voltages of the DPVAnt TFT ($V_{turn\text{-}on}$ = –1.5 V, V_{th} = –1.9 V) are significantly more negative than those for the pentacene TFT ($V_{turn\text{-}on}$ = –0.8 V, V_{th} = –1.4 V).

Based on the difference in the ionization potential (pentacene: 5.0 eV, DPVAnt: 5.4 eV), the DPVAnt devices are expected to degrade less rapidly than the pentacene transistors.

[*] Dr. H. Klauk, Dr. U. Zschieschang, R. T. Weitz
Max Planck Institute for Solid State Research
Heisenbergstr. 1, 70569 Stuttgart (Germany)
E-mail: H.Klauk@fkf.mpg.de
Dr. H. Meng, Dr. F. Sun, Dr. G. Nunes, Dr. D. E. Keys, Dr. C. R. Fincher
Central Research and Development, Experimental Station, E. I. DuPont Company
Wilmington, DE 19880 (USA)
E-mail: Hong.Meng@usa.dupont.com
Z. Xiang
Department of Chemistry, Sichuan University of Science and Engineering
Sichuan 643000 (P.R. China)

[**] The authors thank Benjamin Stuhlhofer at the Max Planck Institute for Solid State Research for expert technical assistance and Richard Rook at CADiLAC Laser for providing high-quality shadow masks.

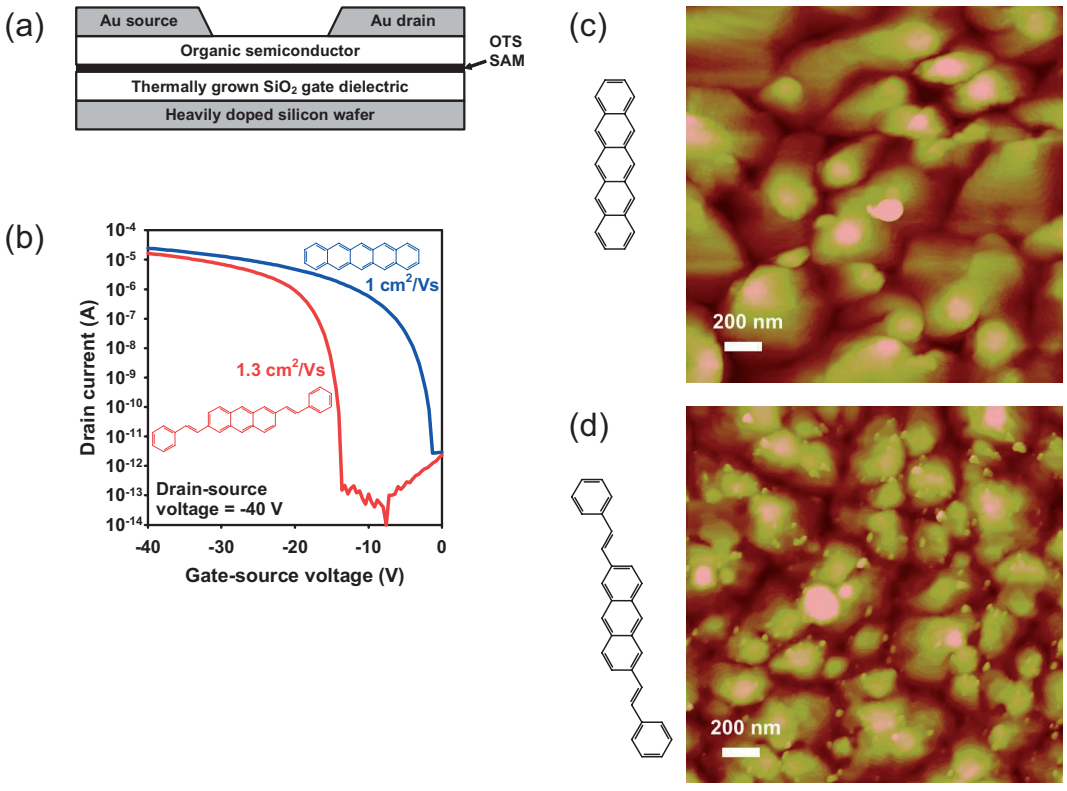

Figure 1. a) Cross section of an organic TFT fabricated on a thermally grown SiO_2 gate dielectric. b) Transfer characteristics of pentacene and DPVAnt TFTs. c) Atomic force microscopy (AFM) image of a pentacene film deposited on OTS-treated SiO_2. d) AFM image of a DPVAnt film on OTS-treated SiO_2. The height in the AFM images ranges from 0 (dark) to 30 nm (light).

To confirm this, we have performed two types of stability tests: a cycle test[12] and a shelf-life test.[4]

Figure 3 shows the electrical characteristics of a pentacene TFT and a DPVAnt TFT during and after a cycle test. During the cycle test a continuous square-wave voltage signal is applied to the gate electrode (with the source contact grounded), a constant drain–source voltage of –1.5 V is applied, and the drain current is monitored using a semiconductor parameter analyzer. The cycle tests have been carried out in air at room temperature, and each transistor has been cycled 10 000 times. As clearly apparent from Figure 3, the electrical response of both TFTs changes during the test. The carrier mobility of the pentacene TFT decreases by more than one order of magnitude (from 0.4 to 0.02 $cm^2\ V^{-1}\ s^{-1}$), and the subthreshold swing degrades from 100 to 240 mV $decade^{-1}$. The threshold voltage of the pentacene TFT remains essentially unchanged (before: –1.4 V, after: –1.3 V).

In contrast to the pentacene TFT, the carrier mobility of the DPVAnt TFT after 10 000 cycles remains exactly the same as before the cycle test (0.3 $cm^2\ V^{-1}\ s^{-1}$). The threshold voltage of the DPVAnt TFT shifts from –1.9 to –2.4 V during the test, thereby reducing the maximum current by about 50%. In addition to the shift in threshold voltage, the subthreshold behavior of the DPVAnt TFT also changes significantly. It appears that there are now two subthreshold regions: one in the gate–source voltage range between –0.5 and –2 V (with a swing of 630 mV $decade^{-1}$) and another in the gate–source voltage range between –2 and –2.5 V (with a swing of 170 mV $decade^{-1}$).

The results of the shelf-life test are shown in Figure 4. During the shelf-life test, the substrates are kept for 100 days in ambient air at room temperature without any protection from relatively weak yellow laboratory lights. It is clear from Figure 4 that the degradation of the transistors during the shelf-life test is similar to the degradation during the cycle test. The mobility of the pentacene TFT decreases from 0.4 to 0.005 $cm^2\ V^{-1}\ s^{-1}$, the subthreshold swing degrades from 100 to 200 mV $decade^{-1}$, and the threshold voltage shifts from –1.4 to –1.1 V. In contrast, the mobility of the DPVAnt TFT is essentially unaffected by ambient air (before: 0.3 $cm^2\ V^{-1}\ s^{-1}$, after: 0.2 $cm^2\ V^{-1}\ s^{-1}$), and the threshold voltage shifts from –1.9 to –1.7 V. As in the case of the cycle test, the subthreshold behavior of the DPVAnt TFT is also significantly modified.

The degradation of organic TFTs in air is usually attributed to an increase in the density of localized trap states in the HOMO–LUMO gap.[1,2] The above-threshold characteristics, especially the carrier mobility, are related to the density of donor states with energy near the HOMO level (shallow

ADVANCED MATERIALS

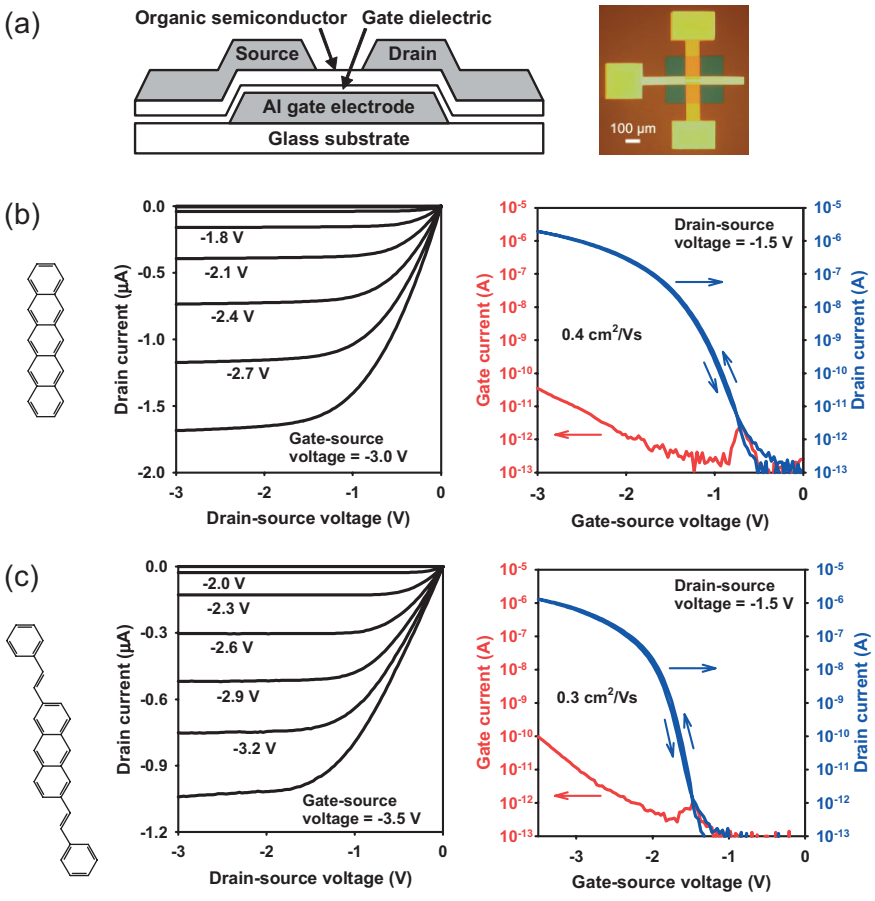

Figure 2. a) Cross section and photograph of an organic TFT with a patterned metal gate. b) Electrical characteristics of a pentacene TFT. c) Electrical characteristics of a DPVAnt TFT. The TFTs have a channel length of 20 μm and a channel width of 100 μm. The current–voltage characteristics have been recorded within 24 h of fabricating the devices.

states).[2] In contrast, the turn-on voltage is affected by acceptor states closer to the middle of the bandgap (deep states).[13,14] The region between the turn-on voltage and the threshold voltage, i.e., the subthreshold swing, is sometimes associated with shallow donor states[13,15] and sometimes with deep acceptor states.[2,15] In our cycle and shelf-life tests, the pentacene TFTs display a significant reduction in mobility, a mild degradation of the subthreshold swing, and only small changes in the turn-on voltage. This suggests that in the case of pentacene most of the trap states generated during degradation are energetically close to the HOMO level (shallow states). In contrast, the mobility of the DPVAnt TFTs is virtually unaffected by the cycle and shelf-life tests, but the subthreshold behavior and turn-on voltage are significantly modified. This suggests that in the case of DPVAnt, most of the generated traps are deep states that do not affect the mobility.

From the cycle and shelf-life tests we conclude that the carrier mobility of the DPVAnt transistors is significantly more stable as compared to that of the pentacene devices. We attribute this to the more negative HOMO energy of DPVAnt (–5.4 eV) as compared to pentacene (–5.0 eV). However, the difference in HOMO energy is also expected to affect the charge injection at the contact/semiconductor interface. Therefore, we have measured the current–voltage characteristics of pentacene and DPVAnt TFTs with channel lengths ranging from 10 to 50 μm, and extracted the contact resistance using the gated transmission line method.[16,17] The results of these experiments are shown in Figure 5a. The width-normalized contact resistance reaches a minimum of 850 Ω cm for the pentacene transistors (gate–source voltage of –3 V, drain–source voltage of –0.1 V) and 1.3 kΩ cm for the DPVAnt transistors (gate–source voltage of –3.5 V, drain–source voltage of –0.1 V). These are both reasonably low values for organic TFTs.[17–23] For both semiconductors the drain current is limited by the resistance of the carrier channel, rather than by the contact resistance, for channel lengths down to 10 μm. Decreasing the channel length below about 8 μm will lead to the channel resistance becoming smaller than the contact resistance, i.e., the transistors will become contact limited.

Considering the significant difference in HOMO energy between the two semiconductors, the difference in contact resistance is smaller than may have been anticipated. This suggests that the carrier-injection efficiency at the contacts is relatively insensitive to the exact position of the HOMO level with respect to the metal Fermi level (in our case the metal is gold with a Fermi level at about –5 eV), at least for the range of HOMO energies considered here (–5.0 to –5.4 eV). This is consistent with the observation that the height of the injection barrier at the metal/organic interface is often significantly modified by interface dipoles.[24] In addition, the widths of the source and drain contact barriers are affected by the gate–source voltage. For large negative gate–source voltages, carrier injection may be dominated by tunneling. Nonetheless, it may be useful to test the influence of a higher work function metal such as platinum on the contacts. However, platinum is not as easily deposited by thermal evaporation and may require electron-beam evaporation, which in turn can have a greater effect on the metal/organic interface properties than the work function of the metal itself. Since thermally evaporated gold provides a reasonably small contact resistance for

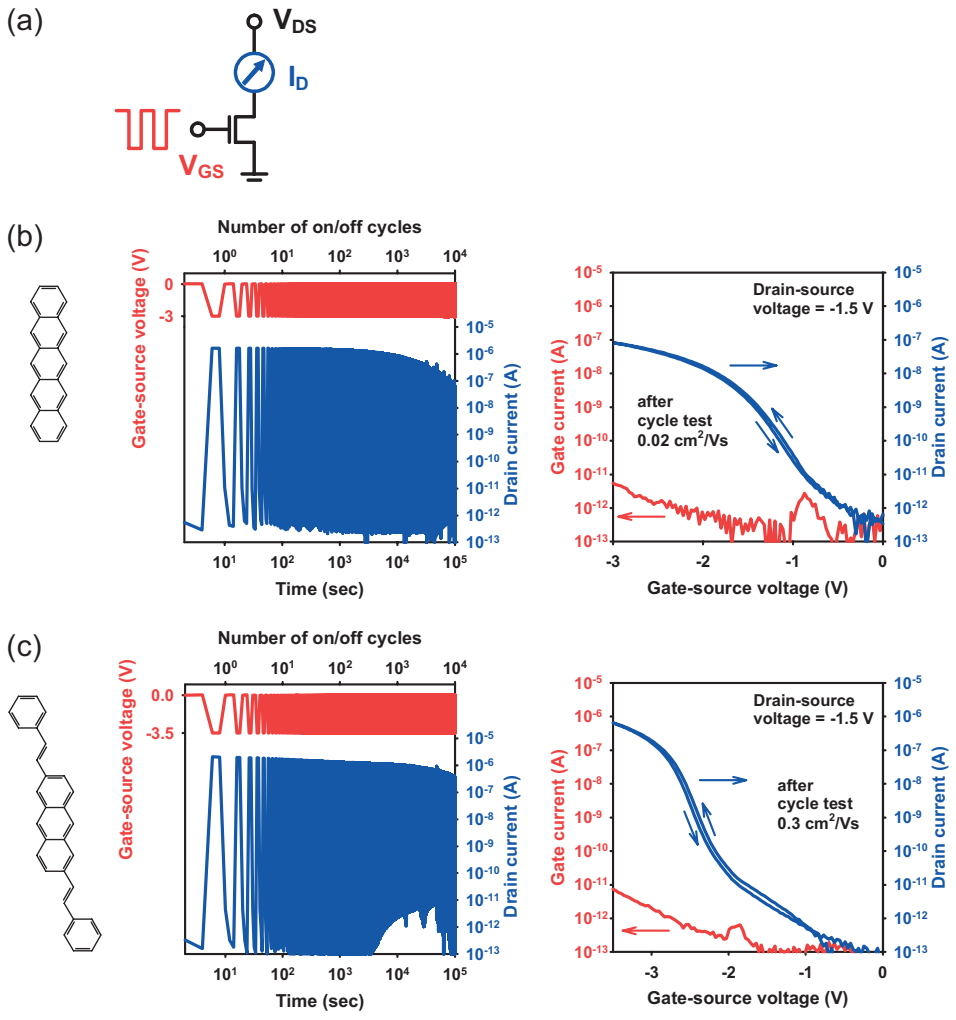

Figure 3. a) Schematic of the cycle test. b) Electrical characteristics of a pentacene TFT during and after the cycle test. c) Electrical characteristics of a DPVAnt TFT during and after the cycle test.

both semiconductors, we have thus far not tested any other contact metals.

To evaluate the dynamic performance of the organic transistors, we have fabricated five-stage ring oscillators based on saturated-load inverters with a channel length of 10 μm, using the same TFT structure and manufacturing process outlined above. Figure 5b shows a schematic and a photograph of the circuit, whereas Figure 5c shows the measured signal propagation delay per stage as a function of the supply voltage. The signal delay per stage at a supply voltage of –5 V is 200 μs for pentacene and 320 μs for DPVAnt. In order to obtain the same signal delay the DPVAnt circuit requires a greater supply voltage than the pentacene circuit (e.g., 400 μs at –3.5 V for pentacene and –4.5 V for DPVAnt). This is mostly owing to the difference in threshold voltage (–1.4 V for the pentacene TFTs, –1.9 V for the DPVAnt TFTs). The minimum supply voltage required to generate oscillation is –2 V for pentacene and –3 V for DPVAnt.

In summary, we have presented a comparison of the static and dynamic performance, as well as the operational and shelf-life stabilities, of organic TFTs based on vacuum-evaporated DPVAnt and pentacene. The carrier mobility, on/off current ratio, subthreshold swing, contact resistance, and ring oscillator delay are all very similar for both semiconductors. However, owing to the larger ionization potential of DPVAnt, the mobility of the DPVAnt transistors is significantly less affected by exposure to air, as compared to pentacene. For commercial applications that require long-term stability under ambient conditions, compounds such as DPVAnt may be more useful than pentacene.

Received: June 14, 2007
Published online: October 31, 2007

[1] J. E. Northrup, M. L. Chabinyc, *Phys. Rev. B: Condens. Matter* **2003**, *68*, 041 202.

ADVANCED MATERIALS

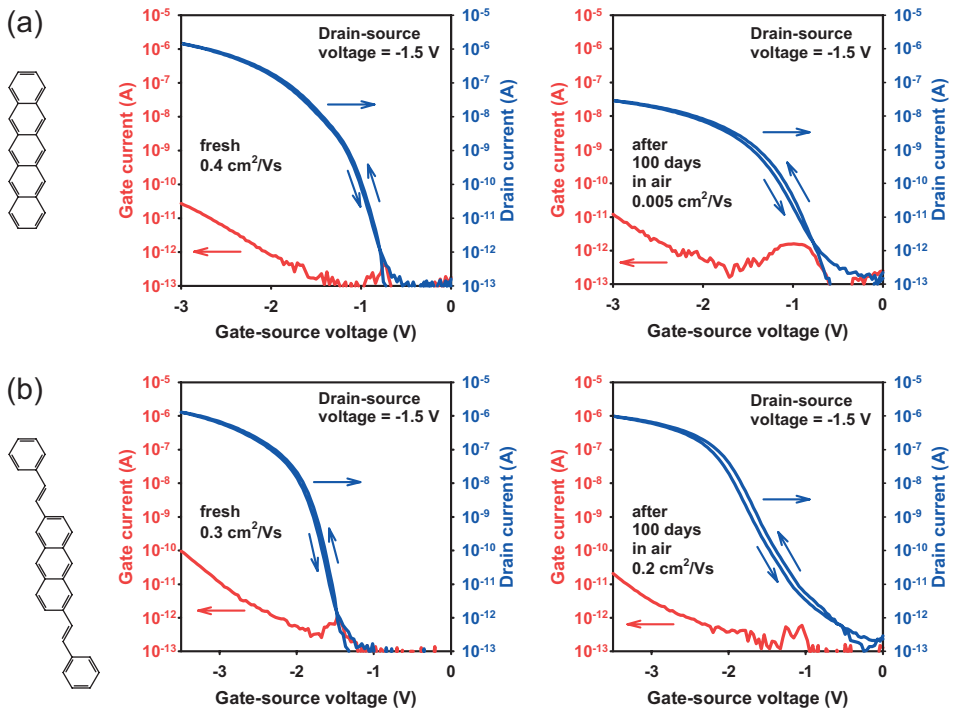

Figure 4. a) Shelf-life stability of a pentacene TFT. b) Shelf-life stability of a DPVAnt TFT.

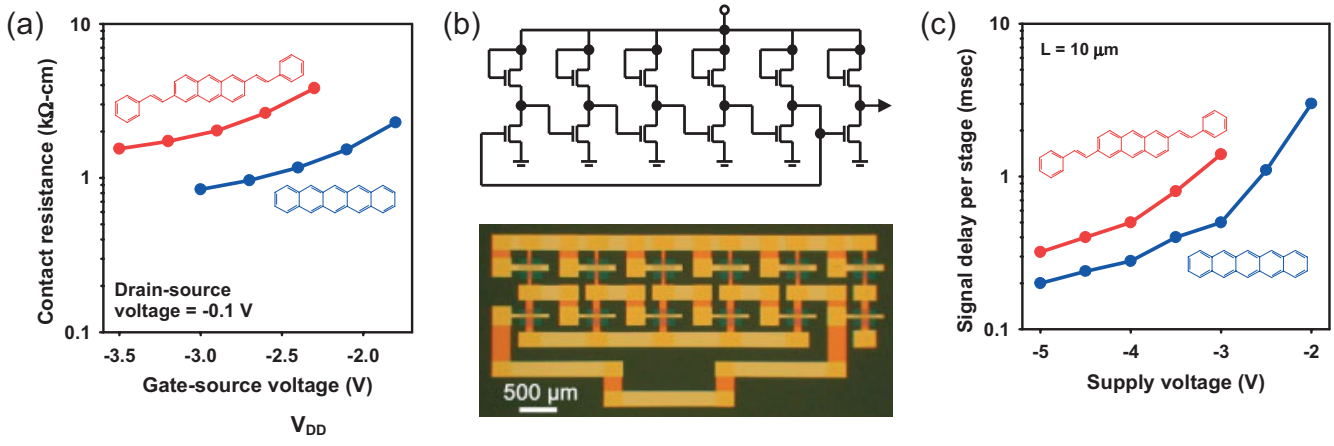

Figure 5. a) Contact resistance determined using the transmission line method as a function of the gate–source voltage for TFTs based on pentacene and DPVAnt. b) Schematic and photograph of a five-stage ring oscillator. c) Signal propagation delay per stage as a function of the supply voltage for ring oscillators based on pentacene and DPVAnt TFTs.

[2] F. De Angelis, S. Cipolloni, L. Mariucci, G. Fortunato, *Appl. Phys. Lett.* **2006**, *88*, 193 508.

[3] H. Meng, Z. Bao, A. J. Lovinger, B. C. Wang, A. M. Mujsce, *J. Am. Chem. Soc.* **2001**, *123*, 9214.

[4] J. A. Merlo, C. R. Newman, C. P. Gerlach, T. W. Kelley, D. V. Muyres, S. E. Fritz, M. F. Toney, C. D. Frisbie, *J. Am. Chem. Soc.* **2005**, *127*, 3997.

[5] S. A. Ponomarenko, S. Kirchmeyer, A. Elschner, N. M. Alpatova, M. Halik, H. Klauk, U. Zschieschang, G. Schmid, *Chem. Mater.* **2006**, *18*, 579.

[6] J. Locklin, M. M. Ling, A. Sung, M. E. Roberts, Z. Bao, *Adv. Mater.* **2006**, *18*, 2989.

[7] H. Meng, F. Sun, M. B. Goldfinger, F. Gao, D. J. Londono, W. J. Marshal, G. S. Blackman, K. D. Dobbs, D. E. Keys, *J. Am. Chem. Soc.* **2006**, *128*, 9304.

[8] M. Koppe, M. Scharber, C. Brabec, W. Duffy, M. Heeney, I. McCulloch, *Adv. Funct. Mater.* **2007**, *17*, 1371.

[9] H. Meng, E. M. Smith, C. H. Hsu, *Int. Patent Application WO2006/113 205*, **2006**.

[10] Y. Y. Lin, D. J. Gundlach, S. F. Nelson, T. N. Jackson, *IEEE Trans. Electron Devices* **1997**, *44*, 1325.

[11] H. Klauk, U. Zschieschang, J. Pflaum, M. Halik, *Nature* **2007**, *445*, 745.

[12] C. R. Kagan, A. Afzali, T. O. Graham, *Appl. Phys. Lett.* **2005**, *86*, 193 505.

[13] D. Knipp, P. Kumar, A. R. Völkel, R. A. Street, *Synth. Met.* **2005**, *155*, 485.
[14] A. R. Völkel, R. A. Street, D. Knipp, *Phys. Rev. B: Condens. Matter* **2002**, *66*, 195 336.
[15] S. Scheinert, G. Paasch, M. Schrödner, H. K. Roth, S. Sensfuß, T. Doll, *J. Appl. Phys.* **2002**, *92*, 330.
[16] H. Klauk, G. Schmid, W. Radlik, W. Weber, L. Zhou, C. D. Sheraw, J. A. Nichols, T. N. Jackson, *Solid-State Electron.* **2003**, *47*, 297.
[17] D. J. Gundlach, L. Zhou, J. A. Nichols, T. N. Jackson, P. V. Necliudov, M. S. Shur, *J. Appl. Phys.* **2006**, *100*, 024 509.
[18] K. P. Puntambekar, P. V. Pesavento, C. D. Frisbie, *Appl. Phys. Lett.* **2003**, *83*, 5539.
[19] J. Zaumseil, K. W. Baldwin, J. A. Rogers, *J. Appl. Phys.* **2003**, *93*, 6117.
[20] B. H. Hamadani, D. Natelson, *Appl. Phys. Lett.* **2004**, *84*, 443.
[21] P. V. Pesavento, R. J. Chesterfield, C. R. Newman, C. D. Frisbie, *J. Appl. Phys.* **2004**, *96*, 7312.
[22] T. Maeda, H. Kato, H. Kawakami, *Appl. Phys. Lett.* **2006**, *89*, 123 508.
[23] P. V. Pesavento, K. P. Puntambekar, C. D. Frisbie, J. C. McKeen, P. P. Ruden, *J. Appl. Phys.* **2006**, *99*, 094 504.
[24] A. Kahn, N. Koch, W. Gao, *J. Polym. Sci., Part B: Polym. Phys.* **2003**, *41*, 2529.

